Accuracy of adenosine-induced stress dynamic myocardial perfusion imaging with dual-source CT : a multicenter trial

Sang A Lee

Department of Medicine

The Graduate School, Yonsei University

Accuracy of adenosine-induced stress dynamic myocardial perfusion imaging with dual-source CT : a multicenter trial

Directed by Professor Byoung Wook Choi

The Master's Thesis
submitted to the Department of Medicine
the Graduate School of Yonsei University
in partial fulfillment of the requirements for the degree
of Master of Medical Science

Sang A Lee

June 2021

This certifies that the Master's Thesis of
Sang A Lee is approved.

Thesis Supervisor : Byoung Wook Choi

Thesis Committee Member#1: Young Jin Kim

Thesis Committee Member#2 : Sak Lee

The Graduate School
Yonsei University

June 2021

ACKNOWLEDGEMENTS

I would like to thank my advisor, professor Choi, who has been an invaluable mentor. His advice have been an inestimable source of support for me during this process. I would also like to thank professor Kim and professor Lee for their advice and feedback. Their varied perspectives have helped me to strengthen my work.

TABLE OF CONTENTS

LIST OF FIGURES

LIST OF TABLES

ABSTRACT

Accuracy of adenosine-induced stress dynamic myocardial perfusion imaging with dual-source CT: a multicenter trial

Sang A Lee

Department of Medicine
The Graduate School, Yonsei University

(Directed by Professor Byoung Wook Choi)

Computed tomography (CT) myocardial perfusion imaging was expected to contribute to the improvement of accuracy in assessing functionally significant coronary stenosis, in addition to the evaluation of anatomically significant stenosis defined by coronary CT angiography (CCTA).

This is a multicenter prospective cohort study performed at four centers. A total of 128 patients participated in this study. Stress and rest perfusion imaging of CT and magnetic resonance imaging (MRI) were performed in 110 and 94 patients, respectively. Of these, 79 underwent perfusion imaging with both CT and MRI and were included in the analysis. The mean age of the patients was 62.3 years. There was a high prevalence of cardiovascular risk factors.

Myocardial blood flow (MBF) and myocardial perfusion reserve (MPR) were different between diseased and non-diseased myocardium. Various combinations of CCTA and CT myocardial perfusion imaging (visual assessment, MBF, and MPR) were found to improve diagnostic accuracy compared to CCTA alone, in diagnosing functionally significant coronary artery disease defined by invasive coronary angiography and MRI perfusion imaging.

CT myocardial perfusion imaging is a useful non-invasive diagnostic method to compensate for the several limitations of CCTA in diagnosing functionally significant coronary diseases and improving diagnostic accuracy. This multicenter study may provide a meaningful basis for the clinical usefulness of CT myocardial perfusion imaging.

Key word: dynamic CT myocardial perfusion imaging

Accuracy of adenosine-induced stress dynamic myocardial perfusion imaging with dual-source CT: a multicenter trial

Sang a Lee

Department of Medicine
The Graduate School, Yonsei University

(Directed by Professor Byoung Wook Choi)

I. INTRODUCTION

Coronary computed tomography angiography (CCTA) has been considered as one of the first-line investigations to exclude coronary artery disease (CAD) in patients with low-to-intermediate risk profile.[1,2] However, interpretation of CCTA is based on the degree of luminal stenosis and has a limitation in determining hemodynamically relevant stenosis, which is crucial for the survival of patients with known CAD[3-5]. Stress myocardial CT perfusion (CTP) is a noninvasive perfusion imaging technique, which could provide functional information of coronary artery stenosis in comprehensive interpretation with CCTA.

There are two types of stress myocardial CTP imaging: static and dynamic CTP imaging. Dynamic CTP imaging is a repetitive image acquisition technique which provides myocardial attenuation changes over time, whereas the static technique obtained a one-shot image at the assumed most hyperemic state. In dynamic CTP imaging, several quantitative parameters such as myocardial blood flow (MBF) or myocardial perfusion reserve (MPR) were calculated directly from time-attenuation curves.

Several studies have documented the diagnostic performance of the combination of CCTA and dynamic CTP compared to various reference standards, such as single-photon emission computed tomography (SPECT),

positron emission tomography (PET), magnetic resonance imaging (MRI), or invasive fractional flow reserve (FFR), but the number of multicenter studies performed to date are insufficient to arrive at a definitive conclusion. This study aimed to determine the diagnostic accuracy of various combinations of CCTA and dynamic CTP with several parameters (visual assessment, MBF, and MPR), through a multicenter trial.

II. MATERIALS AND METHODS

Study population

This study was designed as a prospective cohort study performed at four centers. The study at all four centers was approved by the appropriate institutional review board, and all patients provided written informed consent.

Patients aged 40–80 years, with suspected CAD and scheduled to undergo invasive coronary angiography (ICA) were eligible for enrolment. The exclusion criteria were as follows: clinically unstable conditions; severe heart failure with symptoms (New York Heart Association class III or IV); a history of myocardial infarction or cardiac surgery, including coronary artery bypass graft; known allergy to iodinated contrast media; renal insufficiency [serum creatinine levels > 1.5 mg/dL or estimated glomerular filtration rate (eGFR) < 30 mL/min]; contraindication for beta-blockers; second or third degree atrioventricular block; uncontrolled arrhythmia or atrial fibrillation; claustrophobia; pacemaker insertion status; contraindication for adenosine; hypersensitivity; known or suspected bronchoconstrictive or bronchospastic disease; sinus bradycardia with less than 45 bpm; and systemic arterial hypotension less than 90 mmHg.

Computed tomography, including stress and rest CTP, CCTA, and stress and rest perfusion MRI were performed within 1 month before ICA for comparison.

CTP imaging and CCTA protocol

CT imaging was performed using a second generation dual-source CT system (Somatom Definition Flash, Siemens Healthineers AG), in the order of stress CTP, rest CTP, and CCTA (Figure 1). Before the test, two intravenous routes were secured with an 18-gauge needle in the right antecubital vein and a 20-guage needle in the left antecubital vein for adenosine infusion.

The imaging parameters for stress and rest CTP for both tubes were as follows: voltage of 100 kVp, tube current of 300 mAs/rotation, gantry rotation time of 0.28 s, end-systolically triggered at 35% or 200 ms after R-wave, and dynamic shuttle mode. A test bolus was performed to confirm the acquisition time, using 10 mL of contrast at 5 mL/s (Ultravist 370) with 50 mL saline solution flush. A stress test was first performed in a dynamic CTP study. Acquisition was initiated 5 s before the arrival of the contrast (50 mL at 5 mL/s followed by 30 mL saline chaser) in the ascending aorta after at least 3 min of continuous adenosine infusion (0.14 μg/kg body weight/min). Scanning was continued for 30 s with breath hold, via an electrocardiographically-triggered axial shuttle mode, repeated at two alternating table positions to obtain a Z axis coverage of 73 mm. Data acquisition was performed for every beat if the heart rate (HR) was less than 63 bpm and every second beat if the HR was more than 63 bpm. Adenosine administration was discontinued after data acquisition. A rest CTP was performed at more than 15 min after the stress test, allowing for sufficient washout of the contrast media from the myocardium. It followed the protocol of the stress perfusion test except for the adenosine infusion step.

After dynamic stress and rest CTP, standard prospective CCTA was performed using the following scan parameters: 100-kV or 80-kV tube voltage and 0.28-s gantry rotation time, with injection of 60 mL of contrast medium at 5 mL/s, followed by 50 mL of saline chaser at the same rate. The scan was set to start at a 4 s delay after peak enhancement of the ascending aorta.

During CT examination, blood pressure (BP), HR, and symptoms were monitored and recorded throughout the procedure and up to 10 min after the cessation of adenosine infusion. If there was persistent or symptomatic atrioventricular block, significant drop in systolic BP, persistent or symptomatic hypotension, or severe respiratory difficulty, the adenosine infusion was terminated earlier.

MRI protocol

MRI was performed on a 3-T system (Tim trio, Siemens Healthineers AG), in the order of stress perfusion imaging, rest perfusion imaging, and late gadolinium enhancement (LGE) imaging (Figure 1).

For stress and rest perfusion tests, the saturation recovery imaging with gradient echo protocol was used to acquire the basal, middle, and apical short-axis slices of the left ventricle (LV). The slice thickness was 8 mm and in-plane resolution was less than 3 mm. Same as CT, an intravenous adenosine injection (0.14 mg/kg body weight/min) was continued up to at least 3 min (typically 4–6 min) before stress perfusion image acquisition, to induce hyperemic status of LV myocardium. A bolus injection of contrast media (Gadovist 1.0 mmol/mL, 0.1 mL/kg; Bayer HealthCare Pharmaceuticals) was administered, followed by saline solution flush (30 mL at 5 mL/s). Rest perfusion MRI was performed 10 min after stress perfusion MRI using the same protocol except for adenosine infusion. For LGE, an inversion recovery fast spoiled gradient echo sequence was used at the same three short-axis slices as that of perfusion MRI.

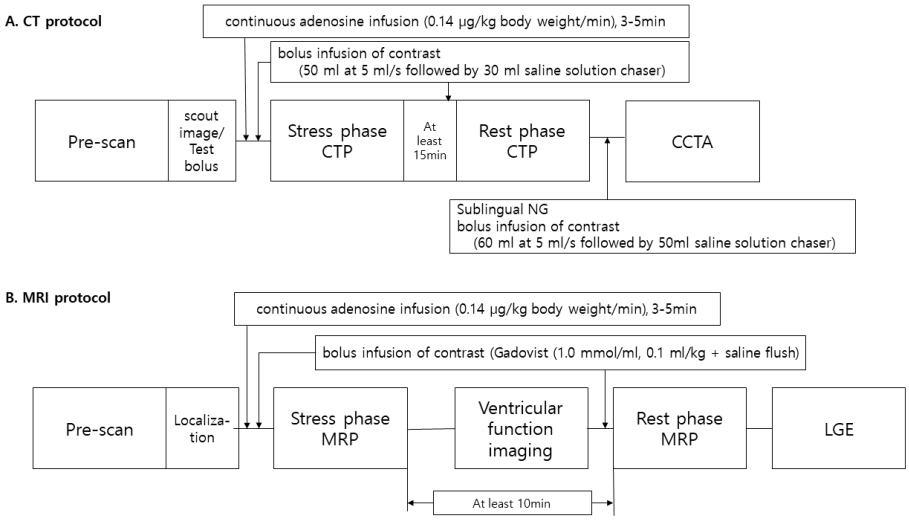

Figure 1. Imaging protocol.

CTP imaging analysis

Dynamic CTP images were analyzed using a commercial software (Syngo VPCT body, Siemens Healthineers AG). Images were reconstructed with a smooth convolution kernel (B30) and a 3-mm slice thickness with 1-mm overlap. The LV myocardium was divided into 16 myocardial segments [according to the American Heart Association (AHA)], excluding an apical segment, in the short-axis view.

All analyses were performed by two reviewers in consensus (with 2 years and 15 years' experience, respectively). For qualitative analysis, perfusion defects in each myocardial segment was visually evaluated in three scales (negative, subendocardial, and transmural). For quantitative analysis, MBF and MPR were measured. MBF was estimated using a dedicated parametric deconvolution technique based on a two-compartment model of the intravascular and extravascular spaces. Insufficiently covered segments or segments severely affected by artifacts were excluded from the analysis. MBF values were obtained from both the stress and rest phase CTP imaging. MPR

was defined as the ratio of stress and rest phase MBF in each myocardial segment.

MRI perfusion imaging and LGE imaging analysis

Presence of hypoperfusion and LGE was visually assessed according to the 16-segment AHA model by the two reviewers in consensus. Both perfusion defect and LGE were recorded in three scales (negative, subendocardial, and transmural).

CCTA imaging analysis

To assess the CCTA images, axial images with 0.75-mm slice thickness, and 0.5-mm section intervals were reconstructed with a medium cardiac kernel. Only vessels with a luminal dimeter of 1.5 mm or more were included in the assessment. Coronary arterial segments were defined using an 18-coronary segment model (modified version of the original 16-segment AHA model). Coronary artery stenosis was evaluated according to the Society of Cardiovascular Computed Tomography guidelines and recorded as a six-point scale: normal = no stenosis, minimal = 1–24% stenosis, mild = 25–49% stenosis, moderate = 50–69% stenosis, severe = 70–99% stenosis, and occlusion. The nonevaluable coronary artery lesions were recorded as positive. More than 50% of luminal stenosis of coronary artery were defined as significant stenosis.

ICA protocol and analysis.

ICA was performed using a 4-Fr or 6-Fr coronary catheter, and the results were interpreted by a cardiologist, who was blinded to the other data. The coronary arterial segments were defined using the 18-coronary segment model, similar to CCTA. The coronary lesions were visually categorized according to their locations in the three vessels [left anterior descending artery (LAD), left

circumflex artery (LCX), and right coronary artery (RCA)] and classified as a 5-point scale: normal = no stenosis, mild = 1–49% stenosis, moderate = 50–69% stenosis, severe = 70–99% stenosis, and occlusion.

Vessel-myocardial territory matching

Vessel-myocardial territory matching was conducted by referring to the algorithm in a previous CORE320 study[6]. Basically, coronary artery segments were grouped into six coronary vessels, namely left main coronary artery (LM), proximal LAD, mid-distal LAD, RCA, LCX, and ramus. Each group has its primary, secondary, and tertiary territories. Primary territories are the anterior and anteroseptal walls of mid to basal LV and entire apical segments for proximal LAD, anterior and anteroseptal walls of mid LV and entire apical segments for mid-distal LAD, lateral and inferolateral walls of mid to basal LV for LCX, inferior and inferoseptal walls of mid to basal LV for RCA, anterior and anterolateral walls of mid to basal LV for ramus, and integration of LAD and LCX territories for LM.

If primary matching was aligned between the location of obstructive coronary lesion and hypoperfused myocardium, there was no need for adjustment. However, if several conditions (such as LM $\geq$ 50% stenosis, ramus $\geq$ 50% stenosis, $\geq$ 50% stenosis within the first 5 mm after the LM bifurcation when a visible ramus branch is present, coronary fistulae, or presence of stent) were present or alignment between the location of obstructive coronary lesion and secondary myocardial vascular territory were noted, adjudication realignment was performed by prespecified rules.

Statistical analysis

All analyses were performed on per-segment, per-vessel, and per-patient bases. At each level of analysis, the diagnostic accuracies of CTP and MRI perfusion imaging were compared using ICA (luminal stenosis >50%) as a reference

standard, and a generalized estimating equation (GEE) was used to determine the p-value. The MBF measured on stress CTP and MPR were compared between functionally significant diseased segments and remote segments, which were determined on perfusion MRI and ICA, using a linear mixed model including random effects for subjects to consider the nature of the clustered data.

Receiver-operating curve (ROC) analysis of the MBF and MPR was performed; the cut-off value of each variable was obtained using Youden's index, and the areas under the ROC curves (AUCs) of each parameter were compared using Delong's method. The sensitivity, specificity, positive predictive value (PPV), negative predicted value (NPV), and overall accuracy of the MBF and MPR were calculated. These analyses were performed at the per-segment level.

The diagnostic performance of CCTA alone and various combinations of CCTA and CTP were measured: CCTA plus CTP (visual assessment), CCTA plus CTP (MBF and MPR, using cut-off value from the ROC curve). The overall sensitivity, specificity, NPV, PPV, and accuracy were calculated for each model and for each level (per-segment, per-vessel, and per-patient). For AUC comparisons of each model in the per-segment and per-vessel analyses, we calculated the nonparametric AUC-type measurements with clustered data and compared the two correlated AUC values. In the per-patient analysis, we used Delong's test for AUC comparisons of each model.

III. RESULTS

A total of 128 patients gave informed consent to participate in this study after screening for inclusion and exclusion criteria. Stress and rest perfusion imaging of CT and MRI were performed in 110 and 94 patients, respectively. Of these, 79 underwent perfusion imaging with both CT and MRI and were included in the analysis (Figure 2). The mean age of the patients was 62.3 years. The percentage of men was 65.8%. There was a high prevalence of

cardiovascular risk factors, which is summarized in Table 1.

Table 1. Characteristics of the study population

Number of patient	79
Age (year)	62.3 ± 9.7
Gender	Male : 52 (65.8%) Female : 27 (34.2%)
BMI (kg/m^2)	25.1 ± 2.90
Cardiovascular risk factors	
Hypertension	41/79 (51.9%)
Dyslipidemia	17/79 (21.5%)
Diabetes	25/79 (31.6%)
Family history of CAD	11/79 (13.9%)
Smoking history (current, past, never)	33(10, 23, 46) (41.8%)
Prevalence of obstructive CAD (ICA > 50%)	
1-vessel disease	20/77 (26.0%)
2-vessel disease	21/77 (27.3%)
3-vessel disease	12/77 (15.6%)
Prevalence of infarcted myocardium*	
Per-segment	78/1248 (6.3%)
Per-vessel	32/234 (13.7%)
Per-patient	15/78 (19.2%)
Prevalence of functionally significant CAD ** (ischemia and infarction)	
Per-segment	161/1232 (13.1%)
Per-vessel	60/231 (26.0%)
Per-patient	37/77 (48.1%)
1-vessel disease	11/77 (14.3%)

2-vessel disease	15/77 (19.5%)
3-vessel disease	11/77 (14.3%)
Prevalence of functionally significant CAD (ischemia only)***	
Per-segment	93/1138 (8.2%)
Per-vessel	35/202 (17.3%)
Per-patient	22/61 (36.1%)

Values are mean ± SD or number with %. BMI = body mass index

* LGE positive segments, LGE positive segment matched vessels, and patient who have at least on LGE positive segment.

** ICA ≥50% luminal stenosis with perfusion defect (defined in MRI perfusion imaging) in the corresponding myocardial region.

*** After excluding prior myocardial infarction, remained myocardial segments, vessels and patients were analyzed

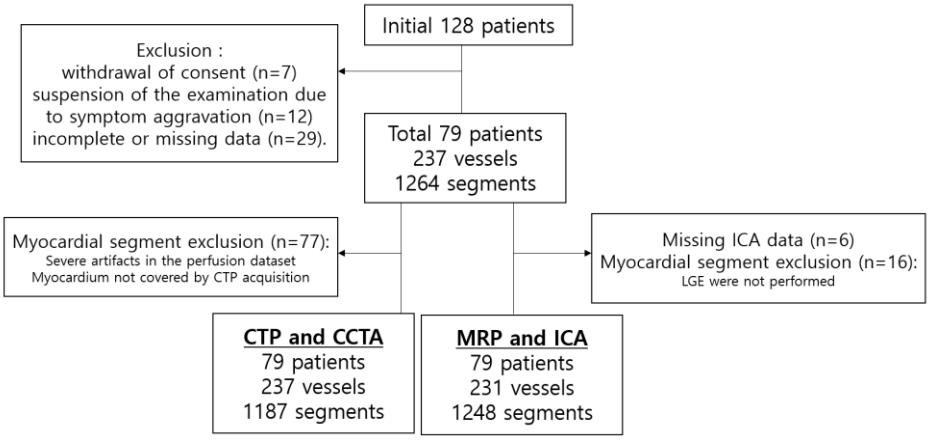

Figure 2. Diagram reporting the flow of participants through the study.

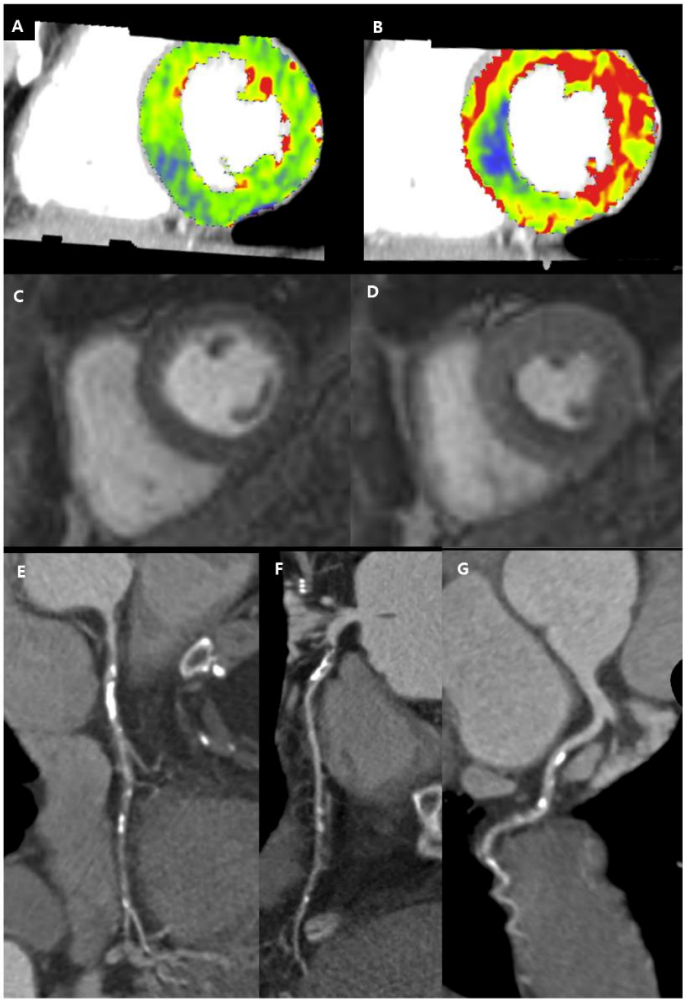

Figure 3. Clinical case.

A 66-year-old man with hypertension and dyslipidemia. (A to D) Dynamic CTP and MRI perfusion imaging showed inducible ischemia in anteroseptal and inferoseptal wall of mid to basal LV, correlated to RCA and LAD territory. Rest CTP (A), stress CTP (B), rest MRI perfusion imaging (C), stress MRI perfusion imaging (D). (E to G) However, CCTA showed three vessel disease, diffuse severe stenosis in proximal to distal RCA (E), severe stenosis in proximal LAD (F) and moderate stenosis in proximal LCx (G).

CCTA and CTP were successfully performed in all patients, but after the exclusion of segments with artifacts or insufficient coverage, 1,204 and 1,238 segments were analyzed for stress and rest CTP, respectively. The number of available segments for both rest and stress images for calculating MPR were 1,187. All segments of stress and rest perfusion MRI were interpretable and available for analysis (each n = 1,264), except for the 16 segments of LGE imaging due to missing data. There were two more patients without ICA data, and a total of 231 vessels were analyzed. The prevalence of functionally significant CAD (both ischemia and infarction) defined by ICA with MRI perfusion imaging was 13.1% for per-segment analysis, 26.0% for per-vessel analysis, and 48.1% for per-patient analysis (Table 1).

CTP and MRI perfusion imaging showed similar diagnostic performances to detect obstructive CAD, at all levels of analysis. The overall accuracy of CTP and MRI perfusion imaging ranged from 0.65 to 0.81 at each level of analysis, without statistically significant differences. However, CTP showed a higher sensitivity and lower specificity than MRI perfusion imaging in per-vessel analysis (0.66 vs. 0.61, p = 0.305 for sensitivity; 0.77 vs. 0.82, p = 0.286 for specificity) and per-patient analysis (0.79 vs. 0.70, p = 0.123 for sensitivity; 0.83 vs. 0.87, p = 0.320 for specificity), but similar sensitivity and specificity in per-segment analysis (0.30 vs 0.30, p = 0.3 for sensitivity; 0.92 vs 0.93, p = 0.261 for specificity) (Table 2).

Table 2-1. Diagnostic performance comparison between CTP and MRI perfusion imaging, for detection of obstructive CAD (per-segment analysis)

	CT	MR	P-value
True positive	161	160	
True negative	639	632	

False positive	53	44	
False negative	379	380	
Sensitivity (95% CI) %	29.81(25.96, 33.67)	29.63(25.78, 33.48)	0.9384
Specificity (95% CI) %	92.34(90.36, 94.32)	93.49(91.63, 95.35)	0.2606
PPV (95% CI) %	75.23(69.45, 81.02)	78.43(72.79, 84.08)	0.1115
NPV (95% CI) %	62.77(59.80, 65.74)	62.45(59.47, 65.43)	0.3622
Accuracy (95% CI) %	64.94(62.27, 67.60)	65.13(62.45, 67.81)	0.5794

Table 2-2. Diagnostic performance comparison between CTP and MRI perfusion imaging, for detection of obstructive CAD (per-vessel analysis)

	CT	MR	P-value
True positive	65	60	
True negative	103	106	
False positive	30	24	
False negative	33	38	
Sensitivity (95% CI) %	66.33(56.97, 75.68)	61.22(51.58, 70.87)	0.3049
Specificity (95% CI) %	77.44(70.34, 84.55)	81.54(74.87, 88.21)	0.2856
PPV (95% CI) %	68.42(59.07, 77.77)	71.43(61.77, 81.09)	0.5007
NPV (95% CI) %	75.74(68.53, 82.94)	73.61(66.41, 80.81)	0.5885

Accuracy (95% CI) %	72.73(66.98, 78.47)	72.81(67.03, 78.58)	0.9433

Table 2-3. Diagnostic performance comparison between CTP and MRI perfusion imaging, for detection of obstructive CAD (per-patient analysis)

	CT	MR	P-value
True positive	42	37	
True negative	20	20	
False positive	4	3	
False negative	11	16	
Sensitivity (95% CI) %	79.25(68.33, 90.16)	69.81(57.45, 82.17)	0.1233
Specificity (95% CI) %	83.33(68.42, 98.24)	86.96(73.19, 100.00)	0.3199
PPV (95% CI) %	91.30(83.16, 99.45)	92.50(84.34, 100.00)	0.5832
NPV (95% CI) %	64.52(47.67, 81.36)	55.56(39.32, 71.79)	0.1477
Accuracy (95% CI) %	80.52(71.67, 89.37)	75.00(65.26, 84.74)	0.2345

MBF and MPR in functionally significant diseased segments defined by ICA and MRI perfusion imaging were lower than those in remote segments ($p < 0.001$ in both), for per-segment analysis. (Table 3). After excluding infarcted segments, MBF and MPR in ischemic segments were still significantly lower than those in remote segments ($p < 0.001$ in both). MBF and MPR were 99.1 mL/100 mL/min and 1.3 in ischemic segments, 90.7 mL/100 mL/min and 1.2 in diseased segments, and 126.3 mL/100 mL/min and 1.6 in remote segments,

respectively. For per-vessel and per-patient analysis, MBF and MPR in functionally significant diseased segments were significantly lower than those of remote segments ($p < 0.001$).

Table 3-1. Comparison of MBF and MPR between non-diseased and diseased segments (per-segment analysis)

	Nondiseased	Diseased*	P-value	Nondiseased	Diseased**	P-value
MBFstr	126.3 ± 37.9	90.7 ± 31.4	p<0.001	126.8 ± 38.1	99.1 ± 30.0	p<0.001
MBFr	82.3 ± 19.3	75.6 ± 15.7	p<0.001	82.8 ± 19.4	79.9 ± 14.0	P=0.015
MPR	1.58 ± 0.43	1.21 ± 0.41	p<0.001	1.58 ± 0.44	1.25 ± 0.34	p<0.001

Table 3-2. Comparison of MBF and MPR between non-diseased and diseased segments (per-vessel analysis)

	Nondiseased	Diseased*	P-value	Nondiseased	Diseased**	P-value
MBFstr	129.1 ± 34.5	98.7 ± 27.2	P=0.019	130.9 ± 34.4	107.4 ± 24.8	P=0.290
MBFr	81.9 ± 17.9	78.7 ± 14.5	P=0.295	82.8 ± 18.0	84.4 ± 11.7	P=0.027
MPR	1.61 ± 0.37	1.27 ± 0.31	p<0.001	1.62 ± 0.38	1.30 ± 0.30	P=0.002

Table 3-3. Comparison of MBF and MPR between non-diseased and diseased segments (per-patient analysis)

	Nondiseased	Diseased*	P-value	Nondiseased	Diseased**	P-value
MBFstr	133.0 ± 35.3	103.9 ± 26.7	p<0.001	133.3 ± 35.7	115.3 ± 21.0	P=0.016

MBFr	83.3 ± 18.8	76,0 13.8	±	P=0.0547	83.8 ± 18.8	81.9 ± 12.1	P=0.646
MPR	1.63 ± 0.38	1.39 0.32	±	P=0.004	1.63 ± 0.38	1.45 ± 0.30	P=0.088

* Diseased : ischemic or infarcted lesion, ** Diseased : ischemic lesion only

MBF = myocardial blood flow; MBFstr = stress phase MBF; MBFr = resting phase MBF; MPR = myocardial perfusion reserve

In ROC analysis for per-segment, AUCs for MBF and MPR to diagnose functionally significant coronary diseases were not significantly different (0.767 and 0.750, respectively; p = 0.634) (Table 4 and figure 4). The cut-off values for MBF and MPR using Youden's index were 99.7 mL/100 mL/min and 1.45, respectively. The sensitivity for MPR was higher than that for MBF (0.81 vs. 0.61). The specificity and PPV for MBF were higher than those for MPR (0.78 vs. 0.60 and 0.29 vs. 0.22, respectively). The overall accuracy of MBF was significantly higher than that of MPR (0.76 vs. 0.62). Sensitivity, specificity, PPV, NPV, and accuracy are summarized in Table 4.

Table 4. Diagnostic accuracy of quantitative parameters (MBF and MPR) and cut-off value for detection of functionally significant CAD.

	MBF	MPR	P-value*
AUC (standard error)	0.767 (0.083)	0.750 (0.079)	0.634
cut-off	99.67ml/100ml/min	1.45	
Sensitivity (95% CI) %	61.33(53.54, 69.13)	80.69(74.26, 87.11)	0.0007
Specificity (95% CI) %	78.14(75.60, 80.67)	59.60(56.58, 62.63)	<.0001
PPV (95% CI) %	29.21(24.18, 34.23)	22.29(18.73, 25.85)	0.0949

NPV (95% CI) %	93.22(91.53, 94.90)	95.56(93.95, 97.16)	0.0142
Accuracy (95% CI) %	75.98(73.54, 78.43)	62.25(59.46, 65.05)	<.0001

* calculated the nonparametric AUC-type measurement with clustered data by referring to Nancy A.obuchowski's method (1997).

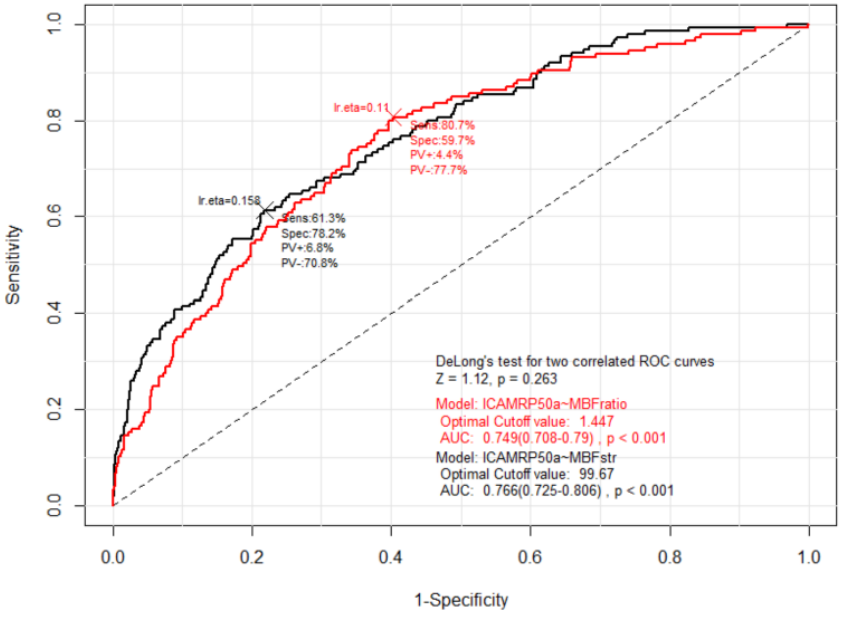

Figure 4. ROC curve for comparison between MBF and MPR.

The diagnostic performance of each model is presented in Table 5. At all levels of analysis, all combinations of CCTA and CTP improved the specificity, PPV, and accuracy compared to CCTA alone. The combination of CCTA with visual assessment of CTP showed the best performance.

Table 5-1. Comparison of diagnostic accuracy of CCTA, CCTA+CTP (visual assessment), CCTA+MBF and CCTA+MPR (per-segment analysis)

	CCTA (>50%LS)	**CCTA+CTP (visual)**	**CCTA+MBFstr (cutoff: 99.67)**	**CCTA+MPR (cut-off:1.45)**
True positive	141	102	77	98
True negative	638	1005	922	833
False positive	433	66	127	207
False negative	20	58	71	46
Sensitivity (95% CI) %	0.88 (0.81, 0.92)	0.64 (0.56, 0.71)	0.52 (0.44, 0.60)	0.68 (0.60, 0.76)
Specificity	0.60 (0.57, 0.63)	0.94 (0.92, 0.95)	0.88 (0.86, 0.90)	0.80 (0.78, 0.82)
PPV	0.25 (0.21, 0.28)	0.61 (0.53, 0.68)	0.38 (0.31, 0.45)	0.32 (0.27, 0.38)
NPV	0.97 (0.95, 0.98)	0.95 (0.93, 0.96)	0.93 (0.91, 0.94)	0.95 (0.93, 0.96)
Accuracy	0.63 (0.61, 0.66)	0.90 (0.88, 0.92)	0.83 (0.81, 0.86)	0.79 (0.76, 0.81)

Table 5-2. Comparison of diagnostic accuracy of CCTA, CCTA+CTP (visual assessment), CCTA+MBF and CCTA+MPR (per-vessel analysis)

	CCTA (>50%LS)	**CCTA+CTP (visual)**	**CCTA+MBFstr (cutoff: 99.67)**	**CCTA+MPR (cut-off:1.45)**
True positive	53	47	40	48
True negative	121	149	145	131
False positive	50	22	25	39
False negative	7	13	19	11
Sensitivity	0.88	0.78	0.68	0.81

(95% CI) %	(0.77, 0.95)	(0.66, 0.88)	(0.54, 0.79)	(0.69, 0.90)
Specificity	0.71 (0.63, 0.77)	0.87 (0.81, 0.92)	0.85 (0.79, 0.90)	0.77 (0.70, 0.83)
PPV	0.51 (0.41, 0.61)	0.68 (0.56, 0.79)	0.62 (0.49, 0.73)	0.55 (0.44, 0.66)
NPV	0.95 (0.89, 0.98)	0.92 (0.87, 0.96)	0.88 (0.83, 0.93)	0.92 (0.87, 0.96)
Accuracy	0.75 (0.70, 0.81)	0.85 (0.80, 0.89)	0.81 (0.76, 0.86)	0.78 (0.73, 0.84)

Table 5-3. Comparison of diagnostic accuracy of CCTA, CCTA+CTP (visual assessment), CCTA+MBF and CCTA+MPR (per-patient analysis)

	CCTA (>50%LS)	**CCTA+CTP (visual)**	**CCTA+MBFstr (cutoff: 99.67)**	**CCTA+MPR (cut-off:1.45)**
True positive	35	32	25	31
True negative	24	32	30	26
False positive	16	8	9	13
False negative	2	5	11	5
Sensitivity (95% CI) %	0.95 (0.82, 0.99)	0.86 (0.71, 0.95)	0.69 (0.52, 0.84)	0.86 (0.71, 0.95)
Specificity	0.60 (0.43, 0.75)	0.80 (0.64, 0.91)	0.77 (0.61, 0.89)	0.67 (0.50, 0.81)
PPV	0.69 (0.54, 0.81)	0.80 (0.64, 0.91)	0.74 (0.56, 0.87)	0.70 (0.55, 0.83)
NPV	0.92 (0.75, 0.99)	0.86 (0.71, 0.95)	0.73 (0.57, 0.86)	0.84 (0.66, 0.95)
Accuracy	0.77 (0.67, 0.86)	0.83 (0.75, 0.91)	0.73 (0.63, 0.83)	0.76 (0.66, 0.86)

The AUCs of all combination models were better than that of CCTA alone (Table 6 and Figure 5). The model of CCTA plus visual assessment of CTP and CCTA plus MBF showed a statistically significant improvement of AUC in the per-segment analysis. In the per-vessel analysis, only CCTA plus visual assessment of CTP showed a statistically significant improvement of AUC. In the per-patient analysis, combination models did not show statistically significant improvement of AUCs compared to CCTA alone.

.

Table 6. AUC comparison results

	M1	Others	P-value
per-segment			
AUC (SE)			
M1 vs. M2	0.818 (0.088)	0.887 (0.097)	0.0051
M1 vs. M3	0.811 (0.086)	0.868 (0.095)	0.0148
M1 vs. M4	0.808 (0.088)	0.850 (0.092)	0.2551
M1 vs. M5	0.806 (0.088)	0.837 (0.091)	0.3486
M4 vs. M5	0.848 (0.092)	0.837 (0.091)	0.5582
per-vessel			
AUC (SE)			
M1 vs. M2	0.860 (0.097)	0.907 (0.106)	0.0381
M1 vs. M3	0.824 (0.094)	0.866 (0.102)	0.1156
M1 vs. M4	0.856 (0.098)	0.876 (0.104)	0.307
M1 vs. M5	0.856 (0.098)	0.890 (0.106)	0.1301
M4 vs. M5	0.876 (0.104)	0.890 (0.106)	0.261
per-patient			
AUC (SE)			
M1 vs. M2	0.868 (0.037)	0.906 (0.031)	0.0702
M1 vs. M3	0.852 (0.043)	0.876 (0.043)	0.2877
M1 vs. M4	0.868 (0.037)	0.878 (0.038)	0.484
M1 vs. M5	0.868 (0.037)	0.873 (0.039)	0.7208
M4 vs. M5	0.878 (0.038)	0.873 (0.039)	0.6743

SE, standard error;

M1= CCTA; M2 = CCTA+CTP(visual assessment); M3 = CCTA+MBF (stress); M4 = CCTA+MPR.

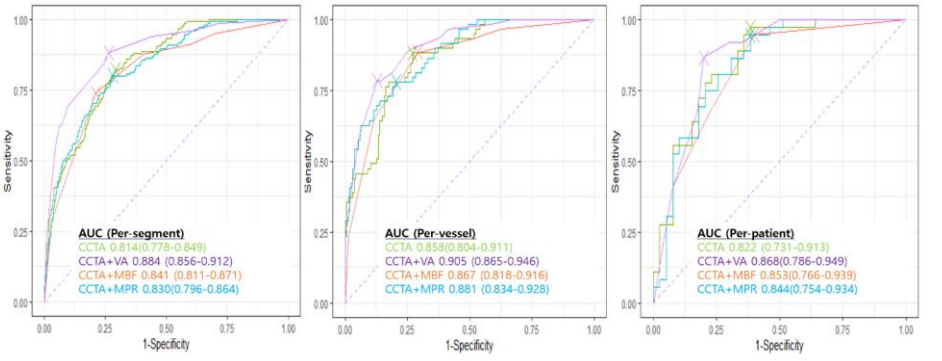

Figure 5. ROC curve for comparison between various combination of CCTA and CTP.

The mean dose-length product for CCTA, stress CTP, and rest CTP were 199.4 ± 146.7 Gycm·cm, 620.6 ± 109.4 Gycm·cm, and 645.4 ± 115.1 Gycm·cm, respectively. The effective doses using converting factor (0.014) were 2.8 ± 2.1 mSV, 8.6 ± 1.8 mSV, and 8.9 ± 1.9 mSV, respectively.

IV. DISCUSSION

This multicenter study demonstrates an incremental diagnostic performance after integration of CCTA and variable parameters of CTP, compared to CCTA alone. The cut-off values for MBF and MPR with moderate accuracy to detect functionally significant CAD were also proposed.

Several previous studies using dynamic CTP reported stress MBF values ranging from 96 to 119.4 5 mL/100 mL/min for ischemic segments and 130 to 137.9 mL/100 mL/min for non-diseased segments[7-9]. However, other studies

showed significantly lower values of stress MBF, ranging from 72.3 to 78.7 5 mL/100 mL/min for ischemic segments and 104.8 to 122.7 mL/100 mL/min for non-diseased segments[5,10-12], or presented much higher values of stress MBF, ranging from 1.37 to 1.5 mL/g/min for ischemic segments and 2.1 to 3.1 mL/g/min for non-diseased segments[13,14]. Based on these results, a wide range of cut-off value (75–103 mL/100 mL/min) to detect myocardial perfusion defect has been reported[5,8,10,12]. In our study, considering all levels of analysis, stress MBF value ranged from 99.1 to 115.3 mL/100 mL/min for ischemic segments and 126.8 to 133.3 mL/100 mL/min for non-diseased segments, with a cut-off value of 99.67 mL/100 mL/min.

MBF value has certain advantages as a quantitative parameter over visual analysis; however, MBF values are affected by various factors, such as imaging techniques (acquisition protocols and post-processing methods)[12], definition of myocardial perfusion defect or coronary obstructive disease with various reference standards (MRI, ICA, FFR, or combined), and characteristics of enrolled patients (age, gender, traditional cardiovascular risk factors, or prevalence of CAD). The wide range of MBF values are attributed to these conditions in each study, and therefore, more data is necessary to define the normal distribution of MBF in healthy subjects from multiple centers.

MPR is conventionally known as coronary flow reserve (CFR) or myocardial flow reserve. Abnormal CFR value results from a complex combination of focal epicardial coronary stenosis, atherosclerotic diffuse coronary stenosis, and microvascular dysfunction[15-20]. As a reference standard for functionally significant stenosis, invasive FFR mostly represents epicardial coronary stenosis, and in cases related to diffuse atherosclerotic narrowing or microcirculatory dysfunction, there could be a discrepancy between FFR and CFR[18]. Several previous studies have suggested CFR as a better prognostic predictor for cardiovascular outcome than invasive FFR[15,20-22].

PET has been considered as a gold standard of non-invasive imaging for CFR. Gould et al.[16] compared more than 250 studies involving approximately 15,000 patients and three different isotopes and reported CFR values in different conditions: 3.55 ± 1.36 for normal controls, 2.02 ± 0.70 for patients with CAD, and 1.93 ± 0.48 for patients with mixed risk factors and known CAD. In contrast, a few studies on CFR derived from CT documented grossly lower CFR values compared to those using PET. Huang et al.[14] revealed a difference in the mean MPR (per-segment base analysis) between the non-ischemic and ischemic groups. Ho et al.[7] performed dynamic CTP in patients with low risk of cardiovascular disease and those with CAD and recorded a CFR of 1.86 ± 0.38 for the low risk group, 1.33 ± 0.27 for the group with ischemia, and 1.33 ± 0.46 for the group with infarction. The result of our study suggested a similar or slightly lower value of MPR compared to previous studies using PET or CT, although the rest MBF value was within the previously documented range. A possible explanation for this result was that the proportion of patients with multivessel disease was higher. The prevalence of three-vessel disease defined as obstructive CAD was 15.6%, and both two- and three-vessel disease was 42.9% in per-patient analysis. In addition, high proportion of severe coronary stenosis, including total occlusion, might influence this result. As considered by coronary collateral steal, MPR less than one is related to severe coronary artery stenosis or occlusion. In our study, there were 125 segments with MPR less than one and 18 vessel territories (26.1% and 20.0% of functionally significant CAD in per-segment and per-vessel analysis, respectively). There are several other factors influencing CFR measurement, such as imaging modality; contrast kinetics, including vasodilating agent; cardiac function (HR and myocardial contractility); and coronary status (serial coronary stenosis, coronary resistance, or coronary collateral circulation)[19,23].

Because measurement of MPR requires both stress and rest phase dynamic CTP

imaging, a higher radiation dose is inevitable compared to other usual protocols without using rest phase dynamic CTP imaging. Increased radiation exposure to patients for acquiring MPR should be carefully considered in clinical practice and is not expected to be easily accepted until the benefit overrules the radiation hazards.

In model-based analysis of our study, AUC was highest in the integration model of CCTA plus visual assessment of CTP, followed by CCTA plus MBF, CCTA plus MPR, and CCTA alone at all levels of analysis. Overall, AUC ranged from 0.806 to 0.907, and highest AUC was recorded in the model of CCTA plus visual assessment of CTP in per-vessel analysis. MBF and MPR, as quantitative parameters, had certain advantages over visual assessment in case of balanced ischemia due to diffuse coronary artery stenosis or subtle myocardial perfusion change beyond visual detection[9,15,16]. However, comprehensive decision could be made by visual assessment, whereas artifacts influenced calculated values. The limitations of vessel-territory matching process also contributed to the better performance of visual assessment. Mismatching of coronary stenosis and myocardial perfusion defect affected the diagnostic performance, which was more pronounced in calculated value.

After the application of CTP parameters, several obstructive CAD lesions defined by CCTA were not hemodynamically significant and were reclassified, resulting in the improvement of overall accuracy. Several previous studies and meta-analyses showed consistent results that additional CTP (mostly MBF value) improved the specificity and PPV compared with CCTA alone[8,24,25]. CCTA has been the first-line modality for exclusion of CAD in patients in the low-to-intermediate risk group because of its high sensitivity and NPV, but it has limitations as a screening tool in patients with known CAD and cohorts with a high prevalence of CAD because of the high false positive rate owing to its low specificity and PPV[2,5]. In addition, extensive coronary calcification,

irregular heartbeat, significant obesity, poor cooperation with breath-hold command, which are often observed in CAD patients, are other obstacles in the diagnosis using CCTA[2]. CTP is a suitable aid to improve the diagnostic performance of CCTA in this condition.

This study has some limitations. First, despite being a multicenter trial, the number of subjects included in this study was relatively small. Second, we used a 64-row detector CT for both rest and stress phase dynamic CTP imaging, and a relatively higher radiation dose was recorded. Currently, wide-detector CT is being used in clinical practice, which dramatically decreases the radiation dose by enabling whole heart coverage.

V. CONCLUSION

This multicenter study demonstrates incremental diagnostic performance after integration of CCTA and variable parameters of CTP, compared to CCTA alone. The model including CCTA plus visual assessment of CTP showed the best performance. The cut-off values for MBF and MPR with moderate accuracy were proposed to detect functionally significant CADs.

REFERENCES

1. Rief M, Chen MY, Lavere AL, Kendziora B, Miller JM, Bandettini WP, et al. Coronary artery disease: analysis of diagnostic performance of CT perfusion and MR perfusion imaging in comparison with quantitative coronary angiography and SPECT— multicenter prospective trial. Radiology 2018;286:461-470

2. Caruso D, Eid M, Schoepf UJ, Jin KN, Varga-Szemes A, Tesche C, et al. Dynamic CT myocardial perfusion imaging. Eur J Radiol 2016;85:1893-1899

3. Pijls NH, Fearon WF, Tonino PA, Siebert U, Ikeno F, Bornschein B, et al. Fractional flow reserve versus angiography for guiding percutaneous coronary intervention in patients with multivessel coronary artery disease: 2-year follow-up of the FAME (Fractional Flow Reserve Versus Angiography for

Multivessel Evaluation) study. J Am Coll Cardiol 2010;56:177–84.

4. Boden WE, O'Rourke RA, Teo KK, B.Ch MB, Hartigan PM, Maron DJ, et al. Optimal medical therapy with or without PCI for stable coronary disease. N Engl J Med 2007;356:1503–16.
5. Greif M, Ziegler FV, Bamberg F, Tittus J, Schwarz F, D'Anastasi M, et al. CT stress perfusion imaging for detection of hemodynamically relevant coronary stenosis as defined by FFR. Heart 2013;99:1004-1011.
6. Cerci RJ, Zadeh AA, George RT, Miller JM, Vavere AL, Mehra V, et al. Aligning coronary anatomy and myocardial perfusion territories, an algorithm for the CORE320 multicenter study. Circ Cardiovasc Imaging 2012;5:587-595.
7. Ho KT, Ong HY, Tan G, Yong QW. Dynamic CT myocardial perfusion measurements of resting and hyperaemic blood flow in low-risk subjects with 128-slice dual-source CT. Eur Heart J Cardiovasc Imaging 2015;16:300-306.
8. Pontone G, Baggiano A, Andreini D, et al. Dynamic stress computed tomography perfusion with a whole-hart coverage scanner in addition to coronary computed tomography angiography and fractional flow reserve computed tomography derived. JACC 2019;12:2460-2471.
9. Meinel FG, Ebersberger U, Schoepf UJ, Lo GG, Choe YH, Wang Y, et al. Global quantification of left ventricular myocardial perfusion at dynamic CT: feasibility in a multicenter patient population. AJR 2014;203:174-180.
10. Bamberg F, Becker A, Schwarz F, Marcus RP, Greif M, Ziegler F, et al. Detection of hemodynamically significant coronary artery stenosis: incremental diagnostic value of dynamic CT-based myocardial perfusion imaging. Radiology 2011;260:689-698.
11. Bamberg F, Marcus RP, Becker A, Hildebrandt K, Bauner K, Schwarz F, et al. Dynamic myocardial CT perfusion imaging for evaluation of myocardial ischemia as determined by MR imaging. JACC 2014;7:267-277.
12. Rossi A, Dharampal A, Wragg A, Davies LC, Geuns RJ, Anagnostopoulos C, et al. Diagnostic performance of hyperaemic myocardial blood flow index obtained by dynamic computed tomography: does it predict functionally

significant coronary lesions? Eur Heart J Cardiovasc Imaging 2014;15:85-94.

13. Huber AM, Leber V, Gramer BM, Muenzel D, Leber A, Rieber J, et al. Myocardium: dynamic versus single-shot CT perfusion imaging. Radiology 2013;269:378-386
14. Huang IL, Wu MT, Hu C, Mar GU, Lee TY, So A. Quantitative low-dose rest and stress CT myocardial perfusion imaging with a whole-heart coverage scanner improves functional assessment of coronary artery disease. Int J Cardiol Heart Vasc 2019;24:100381
15. Taqueti VR, Hachamovitch R, Murthy VL, Naya M, Foster CR, Hainer J, et al. Global coronary flow reserve is associated with adverse cardiovascular events independently of luminal angiographic severity and modifies the effect of early revascularization. Circulation 2015;131:19-27.
16. Gould KL, Johnson NP, Bateman TM, Beanlands RS, Bengel FM, Bober R, et al. Anatomic versus physiologic assessment of coronary artery disease. J Am Coll Cardiol 2013;62:1639–1653.
17. Ko BS, Linde JJ, Ihdayhid AR, Norgaard BL, Kofoed KF, Sorgaard M, et al. Non‐invasive CT‐derived fractional flow reserve and static rest and stress CT myocardial perfusion imaging for detection of haemodynamically significant coronary stenosis. Int J Cardiovasc Imaging 2019;35:2103-2112.
18. Echavarria-Pinto M, Escaned J, Macias E, Medina M, Gonzalo N, Petraco R, et al. Disturbed coronary hemodynamics in vessels with intermediate stenoses evaluated with fractional flow reserve: a combined analysis of epicardial and microcirculatory involvement in ischemic heart disease. Circulation 2013;128:2557-2566.
19. Petretta M, Acampa W, Zampella E, Assante R, Petretta MP, Cuocolo R, et al. Imaging techniques for assessment of coronary flow reserve. Monaldi Arch Chest Dis 2011;76:192-197.
20. Kato S, Saito N, Nakachi T, Fukui K, Iwasawa T, Tauri M, et al. Stress perfusion coronary flow reserve versus cardiac magnetic resonance for known or suspected CAD. JACC 2017;70:869-879.
21. Lee JM, Jung JH, Hwang DY, Park JH, Fan Y, Na SH, et al. Coronary flow

reserve and microcirculatory resistance in patients with intermediate coronary stenosis. JACC 2016;67:1158-1169.

22. Melikian N, Bondt PD, Tonino P, Winter OD, Wyffels E, Bartunek J, et al. Fractional flow reserve and myocardial perfusion imaging in patients with angiographic multivessel coronary artery disease. JACC 2010;3:307-314.
23. Vasu S, Bandettini WP, Hsu LY, Kellman P, Leung S, Mancini C, et al. Regadenoson and adenosine are equivalent vasodilators and are superior than dipyridamole- a study of first pass quantitative perfusion cardiovascular magnetic resonance. JCMR 2013;15:85.
24. Nishiyama H, Tanabe Y, Kido T, Kurata A, Uetani T, Kido T, et al. Incremental diagnostic value of whole-heart dynamic computed tomography perfusion imaging for detecting obstructive coronary artery disease. Journal of Cardiology, 2019;73:425-431.
25. Lu M, Wang S, Sirajuddin A, Arai AE, Zhao S. Dynamic stress computed tomography myocardial perfusion for detecting myocardial ischemia: a systematic review and meta-analysis. Int J Cardiol 2018;258:325-331.

ABSTRACT(IN KOREAN)

이중선원 전산화단층촬영을 이용한 아데노신 유발의 스트레스 동적 심근관류영상: 다기관 임상시험

<지도교수 최 병 욱 >

연세대학교 대학원 의학과

이 상 아

본 다기관 연구는 동적 CT 관류 영상을 시행하여 얻은 정량 분석 수치, 즉 심근 혈류 (myocardial blood flow, MBF) 와 심근 관류 예비량 (myocardial perfusion reserve, MPR)을 분석하였다, 이 수치들이 기능적으로 유의미한 관상동맥 질환으로 인한 심근 허혈 혹은 경색 상태와, 질환이 없는 심근 사이에 유의미한 차이가 있음을 확인하였고, 두 상태를 가름할 수 있는 기준 값을 다기관 데이터를 바탕으로 제시하였다. 이후 CT 관상동맥 조영술과 CT 심근 관류영상 (시각적 정성평가, MBF 및 MPR 정량 평가 수치)의 다양한 조합으로, 기능적으로 유의미한 관상동맥 질환을 진단하는데 있어, CT 관상동맥 조영술 단독에 비하여 정확도가 향상됨을 확인하였다.

CT 심근 관류 영상은 기능적으로 유의미한 관상동맥 질환을 진단하는데 있어 CT 관상동맥 조영술의 단점을 보완하고, 진단 정확도를 향상시키는 데 있어 유용한 비침습적 진단 방법이다. 본 다기관 연구는 CT 심근 관류 영상의 임상적 유용성에 관하여 의미 있는 근거가 될 수 있을 것으로 생각된다.

핵심되는 말 : 동적 CT 관류 영상